

Article

# Harnessing green chemistry for waste water remediation through *Alpinia* leaves silver nanoparticles

Mathivathani Kandiah\*, Rathnayake P. Rathnayake, Beneli Gunaratne, Ominda Perera

School of Science, Business Management School, Colombo 00600, Sri Lanka

\* **Corresponding author:** Mathivathani Kandiah, [mathi@bms.ac.lk](mailto:mathi@bms.ac.lk)

## CITATION

Kandiah M, Rathnayake RP, Gunaratne B, Perera O. Harnessing green chemistry for waste water remediation through *Alpinia* leaves silver nanoparticles. *Pollution Study*. 2024; 5(2): 3005.  
<https://doi.org/10.54517/ps.v5i2.3005>

## ARTICLE INFO

Received: 16 October 2024  
Accepted: 14 November 2024  
Available online: 11 December 2024

## COPYRIGHT



Copyright © 2024 by author(s).  
*Pollution Study* is published by Asia Pacific Academy of Science Pte. Ltd. This work is licensed under the Creative Commons Attribution (CC BY) license.  
<https://creativecommons.org/licenses/by/4.0/>

**Abstract:** Addressing environmental concerns with sustainable nanomaterial is a vital step towards innovative and eco-friendly techniques that address important global issues like pollution, water contamination, and resource depletion. This eco-friendly approach offers a sustainable alternative to conventional methods and this study aims to showcase the applications of biogenic silver nanoparticles (AgNPs) synthesized using green synthesis techniques with aqueous leaf extracts from five *Alpinia* varieties; *Alpinia purpurata*, *Alpinia caerulea*, *Alpinia zerumbet* 'variegata', *Alpinia calcurata* and *Alpinia zerumbet*. The AgNPs were synthesized using water extracts (WE) and silver nitrate at the optimum conditions. Characterization of AgNPs using UV-Vis spectroscopy and scanning electron microscopy (SEM), confirmed their successful formation and morphology. Spherical *A.zerumbet*\_AgNPs between 28–68 nm in size were observed. The photocatalytic activity was tested by degrading methyl Orange (MO) dye under solar irradiation and the use NaBH<sub>4</sub> with AgNPs significantly increased the degradation of MO. P-nitrophenol catalysis using AgNP and NaBH<sub>4</sub> resulted promising results. Cytotoxicity of AgNPs using *Artemia salina* was evaluated and 100% viability was seen. The antibacterial activity was conducted using *Escherichia coli* and *Staphylococcus aureus*, unlike the WEs, all AgNPs showed antibacterial activity. This study revealed that the AgNPs synthesized using *Alpinia* leaves has diverse functional properties, presenting a promising avenue for future research and practical applications in environmental pollution.

**Keywords:** green synthesis; silver nanoparticles; photocatalytic; para-nitrophenol; environmental remediation; cytotoxicity; antibacterial; pollution

## 1. Introduction

Environmental pollution has become a major issue worldwide due to high population and rapid industrialization. The main challenge would be addressing the contamination of drinking water sources by effluents such as pharmaceuticals, pesticides, organic dyes and detergents [1]. Many conventional remediation techniques have been implemented nevertheless, their inherent limits and downsides, including low efficiency, difficult process and high operating costs are the main reasons for their failure in many developing countries with limited finances [2]. To address the limitation of current treatment procedures, researchers have focused on using nanomaterials as an alternate strategy with the advancement of nanotechnology.

Nanotechnology is an essential field of contemporary research that focuses on the synthesis, design, and control of the size and structure of particles. These processes take place at the minuscule nanoscale [3]. There are two methods for synthesising nanoparticles: top-down and bottom-up methods. The “top-down” technique depends on the sequential processing or fragmentation of macro-scale materials to smaller

nano-sized items, whereas the “bottom-up” technique builds nanoscale materials by assembling atoms and molecules [4].  $\text{Ag}^+$  ions are reduced into  $\text{Ag}^0$  during the chemical production of silver nanoparticles (AgNPs) using chemical reducing agents which involves unwanted usage of dangerous chemicals and the resulting AgNPs are less biocompatible. Currently, the majority of nanoscale metals are produced using chemical, physical and biological methods, which are not sustainable and might have unforeseen consequences. Biological methods involve bio-reduction using microorganisms to synthesize AgNPs. However, the microbiological technique has limitations, including biohazard, longer time consumption and maintaining cultures [5].

Green synthesis, which utilises plant extracts is less expensive, produces less pollution, and enhances the safety of the environment and human health, it is preferable to traditional chemical synthesis [6]. AgNPs have attracted increasing interest because of their high conductivity, chemical stability, localised surface plasma resonance, catalytic activity, and antioxidant activity. Studies have discovered phytochemicals in plants, including flavonoids, anthocyanins, and phenolic compounds which have antioxidant properties [7]. Using plant-extracted antioxidants as reducing agents allow green synthesis of nanoparticles which aims to minimize waste generated and implementing sustainable processes by using mild reaction conditions and nontoxic precursors promoting environmental sustainability [8].

*Alpinia* sp. are important *Zingiberaceae* family medicinal plants used in Ayurveda medicine, mainly the rhizome. It is a perennial herb that grows widely in Sri Lanka, India, China and other Southeast Asian nations with accounts indicating of its use for centuries [9]. Numerous therapeutic properties of the plant, including anti-inflammatory, antiallergic, antifungal, antibacterial, and antidiabetic properties, have been discovered from the research done on the plant rhizomes but the leaves are not much studied [10]. Similar study done on multiple plant parts of *Alpinia galanga* L. discovered high phytochemical content (terpene, phenolic, and alkaloid groups), which exhibits a wide range of bioactivities such as antibacterial and antioxidant activity [11]. Thereby this plant can be used to its maximum potential with its implementation in synthesising nanomaterials.

Mainly the textile industry uses azo dyes, such as Congo red and methyl orange (MO), frequently posing a risk to aquatic life and human health due to high toxicity and carcinogenicity [12]. Improper disposal of textile effluents negatively impacts the environment by decreasing oxygen levels in water bodies and reducing solar radiation, which in turn diminishes the photosynthetic activity of aquatic plants and algae [13]. The high stability and limited biodegradability of these dyes can complicate remediation efforts. Conventional physical and chemical methods are hazardous, while using microorganisms are not efficient. Therefore, most suitable method in treating dye effluents is photocatalysis using AgNPs, where the valence band (VD) electrons are excited by light irradiation to the conduction band (CD). The free radicals produced in this process completely breaks down the dye into non-toxic byproducts like  $\text{CO}_2$  and  $\text{H}_2\text{O}$  [14].

Para-nitrophenol (PNP) is a nitroaromatic compound used as the precursor in the production of insecticides, explosives, pharmaceutical drugs, and synthetic colours [15]. That is toxic due to its stability and solubility in wastewater and the conventional

degradation methods using heavy metal catalysts are hazardous [16]. Studies have shown that PNP contaminated water can pose a threat to both aquatic and land organisms. Japanese Quails that ingested PNP-polluted water were observed to exhibit significant hepatocyte degeneration and haemolysis of red blood cells [17]. *Larimichthys crocea*, which is an economically important marine fish species, has shown severe damages and histological changes in gills, renal and liver cells when exposed to high PNP concentrations even for 96 h [18]. PNP is a very important compound as it is a key component in the industrial synthesis of acetaminophen (paracetamol), a widely used analgesic. The frequent use of pesticides and the drugs that wind up in landfills are thought to be two of the main sources of PNP found in the environment [19]. Due to its large-scale use and the severe toxicity U.S. Environmental Protection Agency has classified PNP as both a hazardous waste and a priority toxic pollutant [20]. AgNPs are utilized to reduce the activation energy barrier in the catalytic reduction of PNP using  $\text{NaBH}_4$ , where the reaction is too slow due to the presence of kinetic barrier. AgNPs overcome this kinetic barrier by facilitating the electron transfer and adsorption of p-nitrophenolate ions on the AgNPs surface [21]. The catalytic reduction product, para-amino phenol (PAP) is less toxic than PNP and used for the production of some drugs.

The process of developing new antibiotics is challenging and time-consuming, requiring years of research. Meanwhile, AgNPs and other nanomaterials have been investigated in an effort to find novel agents that can aid in the fight against pathogenic microbes without encouraging the emergence of new resistances [22]. According to several studies, the AgNPs penetrate cells, produce reactive oxygen species (ROS), create free radicals, and inactivate proteins within the cell causing damage to the bacterial cell [23]. Antibacterial susceptibility test (ABST) is crucial especially done on both Gram-positive (*S. aureus*) and Gram-negative (*E. coli*) bacteria as they respond differently to AgNPs, due to differences in their cell wall structure [24]. Positive antibacterial activity suggest that AgNPs are potential alternatives for addressing microbial resistance being used in medical devices and antimicrobial coatings on top of water treatment [25].

Several studies have suggested that these antimicrobial effects of AgNPs have a potential to be cytotoxic to other organisms even mammalian cells. In this regard AgNPs being a double-edged sword, it is essential to ensure that it has minimal to no toxic effect acceptable to be used in the environment [26]. Cytotoxicity studies are useful as a first step in determining the potential toxicity of a test material, such as plant extracts or physiologically active compounds derived from plants. The cytotoxicity effects of AgNPs were investigated using *Artemia salina* (Brine Shrimps) due to its testing rapidity, convenience, and low cost [27]. It is a small aquatic crustacean that lives in saline environments that is highly sensitive to environmental changes due to pollutants. The life cycle of *Artemia salina* has a cyst stage (dormant eggs) that hatches into free swimming larvae within 24 h, which is mainly used in acute cytotoxicity testing [28]. A lower survival rate indicates higher toxicity of the substance being tested.

This study aims to investigate the possibility of producing AgNPs from the leaves of various *Alpinia* varieties. Using MO dye, photocatalytic activity will be evaluated by subjecting it to sunlight and a catalyst. Furthermore, the PNP catalysis activity of

the synthesized AgNPs was evaluated. The antibacterial properties will be tested against *Escherichia coli* and *Staphylococcus aureus*. The cytotoxicity analysis for the synthesized AgNPs is done using brine shrimps for evaluating the safety to be used in the intended applications. The SEM imaging will be one for determining the nanoparticle size and shape. The purpose of this work is to investigate the production of biogenic AgNPs utilising *Alpinia* leaf extracts, as well as their multifunctional uses, in order to provide a sustainable, eco-friendly solution for tackling key environmental pollution.

## 2. Materials and methods

### 2.1. Sample collection

Five varieties of *Alpinia* (**Figure 1**) were found on the Henarathgoda Botanical Garden, Gampaha. The collected leaves were cleaned to remove impurities and stored in labelled zip-lock bags.



**Figure 1.** Varieties of *Alpinia* sp. (A) *Alpinia purpurata* (*A.purpurata*\_AgNP); (B) *Alpinia caerulea* (*A.caerulea*\_AgNP); (C) *Alpinia zerumbet* ‘variegata’ (*A.zerumbet*(V)\_AgNP); (D) *Alpinia calcurata* (*A.calcurata*\_AgNP); (E) *Alpinia zerumbet* (*A.zerumbet*\_AgNP).

### 2.2. Preparation of leaf water extracts (WE)

The sample was dried for 48 h in the dry oven at 40 °C and then cut into small pieces. 2 g of it was then mixed with 50mL of distilled water (DW) and incubated at 99 °C for 30 m. WE was obtained by filtering off using Whatman filter paper 01, it was stored at 4 °C for future use [29].

### 2.3. Synthesis of AgNPs

1 mL of WE was mixed with 9 mL of 1 mM Silver nitrate ( $\text{AgNO}_3$ ). The samples were incubated at 60 °C and 90 °C for 15, 30, 45 and 60 min and at room temperature (RT) for 24 h. They were then stored at 4 °C until further use [30].

### 2.4. Characterization of AgNP using spectrophotometry and SEM.

The absorbance values was taken from 340–520 nm using the UV-Visible spectrophotometer in plastic cuvettes using DW as the blank to confirm the formation of AgNPs

1 mL of *A.zerumbet(V)*\_AgNP was centrifuged at 12,000 rpm for 1 min and repeated until a prominent pellet appears while discarding the supernatant. The pellet was oven dried at 40 °C to remove any remaining liquid. The sample was gold coated using a sputter coater before analysis. The analysis was performed in Sri Lanka Institute of Nanotechnology (SLINTEC) using HITACHI SU6600 SEM.

## 2.5. Catalytic activity of AgNP

### 2.5.1. Photocatalytic activity-Degradation of MO using AgNPs

MO dye of concentration 1ppm was prepared and the absorbance values of it was measured from 350–530 nm. To 100 mL of 1ppm MO dye was prepared in a beaker and 1mL of 4000 ppm AgNP sample was added and kept under sunlight. Readings were taken from 350–530 nm every 15 min for 120 min using DW as the blank. This procedure was carried out for all concentrated and diluted AgNP samples of 267 ppm concentration. The same procedure was repeated to all AgNP samples with the addition of 1mL of 0.2 M NaBH<sub>4</sub> with 100 mL of 1ppm MO dye and 1mL sample. This was done for both 4000 ppm and 267 ppm concentrations of each AgNP sample. Readings were then taken from 350–530 nm every 10 min until a flat line was observed in the absorbance graph, using DW as blank [31].

### 2.5.2. PNP degradation by AgNPs

The catalytic activity of AgNPs against PNP was determined by the reduction of the peak in the 380–420 nm range and the formation of the end product called PAP with the peak at 300 nm, compared to the PNP control. Separately 10 ppm PNP and 600 ppm NaBH<sub>4</sub> solutions were prepared. Three mixtures were created in quartz cuvettes: one with 3 mL of PNP, another with 1 mL of PNP and 2 mL of NaBH<sub>4</sub>, and the last with 1 mL of PNP, 2 mL of NaBH<sub>4</sub>, and 20 µL of AgNPs. The absorbance values for all three mixtures from 280–500 nm were measured in a UV-Visible spectrophotometer using DW as blank at 5-min intervals for 30 min [32]. This procedure was repeated for all four AgNP samples.

## 2.6. Cytotoxic assessment

*Artemia Salina* (Brine shrimp) eggs were grown in sea water for 24 h using an aerator and a yellow lamp. Two dilutions of AgNPs (40 mg/mL and 10 mg/mL) were made with filtered sea water. Into the wells of the 96 well plate, 200 µL of the dilutions and 2 shrimps were added and kept for 24 h under the yellow light. This was done in triplicates and for the control 2 shrimps and filtered sea water were added [33]. The viability was calculated using the Equation (1).

$$\text{Viability} = \frac{\text{Number of viable shrimps} - \text{Number of non-viable shrimps}}{\text{Number of Viable shrimps}} \times 100 \quad (1)$$

## 2.7. Antibacterial susceptibility test (ABST)

The Muller-Hilton agar was prepared by boiling and autoclaving at 121 °C for 15 m. After the agar was cooled, they were poured into labeled agar plates. *E. coli* and *S. aureus* inoculums were streaked onto the agar surface using a cotton swab. Sterilized pipette tips were used to punch holes to load the samples (S1 and S2) and the negative

control. 1 mL of AgNPs and WEs were placed in a watch glass and kept in the dry oven at 40 °C until it evaporated. AgNPs and WE samples were added to S1 and S2 wells. 0.9% saline and gentamycin disc were used as negative and positive controls, respectively. The plates were incubated for 24 h, and the zone of inhibition (ZOI) was recorded.

### 3. Results and discussion

Biogenic AgNPs synthesized using non-toxic low energy processes offers several advantages over the conventional methods. This study's goal was to create AgNPs utilizing five different *Alpinia* varieties and assess their photocatalytic activity, antimicrobial properties and cytotoxicity for the use in bioremediation and other environmental applications. To circumvent issues seen in traditional approaches like hazardous chemicals, high energy usage, and costly expenses green synthesis methods were used. The plant extracts were prepared utilizing water as the solvent, which makes the process convenient and environmentally friendly, allowing the potential for green and sustainable processing [34].

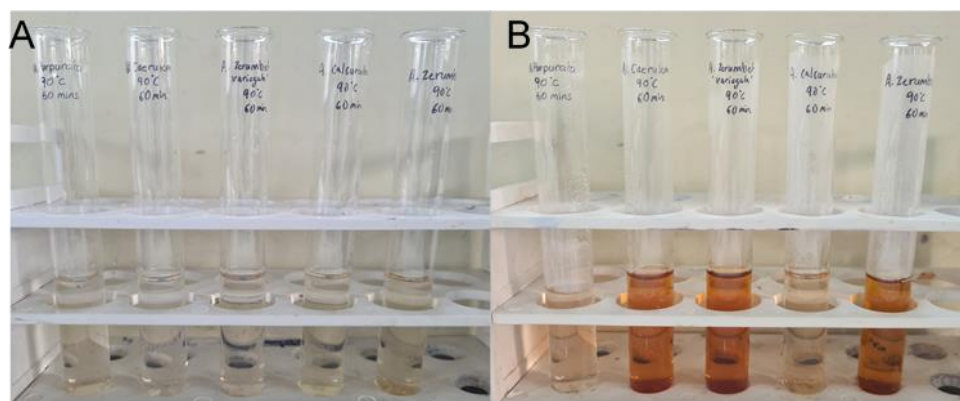
#### 3.1. Synthesis of AgNP

The antioxidant compounds present in the plant water extract reduces metal salts from positive ( $\text{Ag}^+$ ) to a zero ( $\text{Ag}^0$ ) oxidation state. Then these biomolecules also serve as a stabilizer preventing the agglomeration of the nanoparticles by forming a monolayer on the surface of nanoparticles. The presence of a strong reductant in the extract promotes a fast reaction rate and favors the formation of smaller nanoparticles [35].

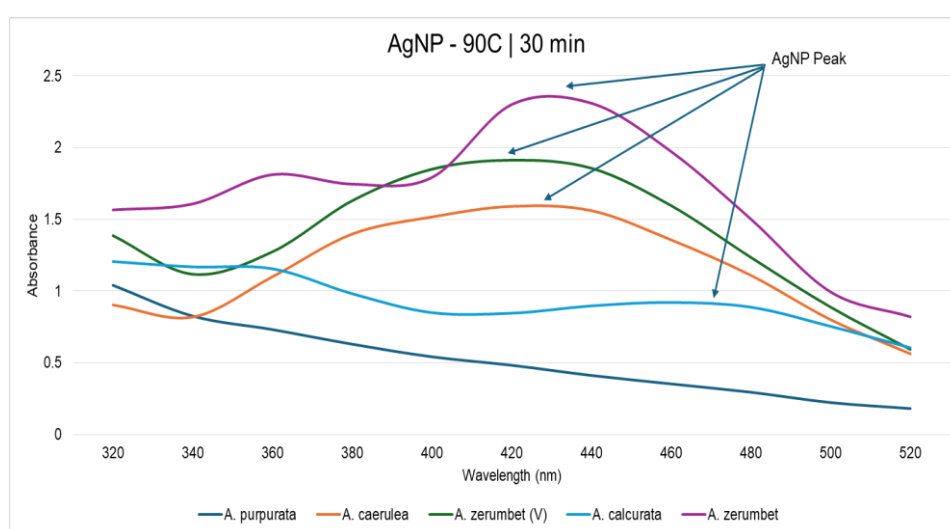
AgNPs specially have features like the localised surface plasma resonance (SPR) that vary according to their size and morphologies [36]. When light photons interact with the AgNPs surface, the outer free electrons of the particles form localized plasmons, which are density waves of the free outer electrons. Incidence of specific wavelengths of light cause the outer electrons to oscillate. This event is called SPR. Due to these resonances; the absorption and scattering intensities are much greater than those of the same particles without plasmonic features [37].

#### 3.2. Characterization of AgNP

The presence of AgNP is observed as a brown colour change after incubation of  $\text{AgNO}_3$  with the WEs (**Figure 2**) along with the absorbance peaks observed at 420 nm (**Figure 3**). According to a study carried out in 2015, using *Alpinia calcurata* WE, the prominent absorbance peak for synthesized AgNP using silver nitrate was observed at 425 nm [38].



**Figure 2.** Before (A) and after (B) incubation at 90 °C for 30 m.

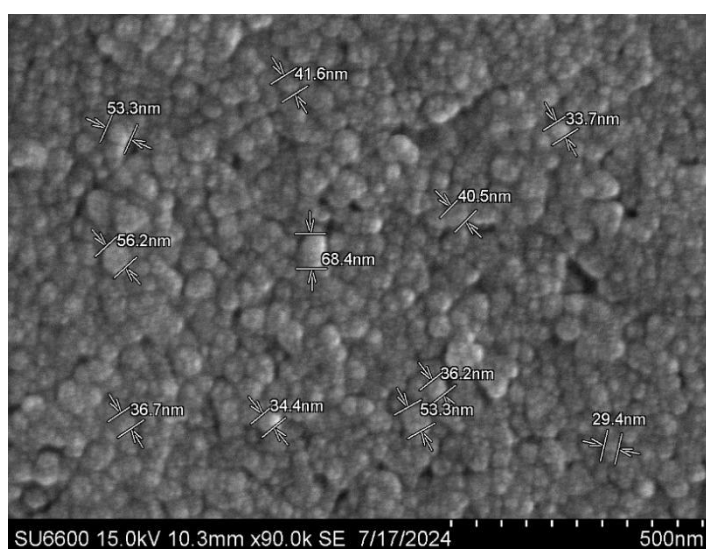


**Figure 3.** Absorbance vs. wavelength (nm) graph of 90 °C 30 min showing AgNP peak.

According to the AgNP synthesis optimization results given in **Table 1**, AgNP were only detected in 4 out of the 5 samples at 90 °C and 60 °C for 30 and 40 m. But the optimum temperature and time was selected as 90 °C-30 minutes as it showed the highest absorbance peak as seen in **Figure 4**, indicating a higher concentration of AgNPs. The rate of AgNP synthesis using plant extracts significantly increases with temperature (30–90 °C), which also results in the creation of small-size NPs [39]. The hypothesis as to why particle size decreases with temperature is with high reaction rate most silver ions are consumed in the formation of nuclei, thus terminating the secondary reduction process on the surface of the created nuclei [39,40]. This was seen in a study done with using 1mM silver nitrate and *Magnolia* leaf extract, where only 11 m was taken for 90% progression of AgNP synthesis at 95 °C and the average particle size decreased from 50 nm at 25 °C to 16 nm at 95 °C in the AgNP synthesis done with *Diopyros kaki* leaf extract [40].

**Table 1.** Optimization table of AgNPs (√—synthesized, x not synthesized).

Temp/Time	<i>A. purpurata</i>	<i>A. caerulea</i>	<i>A. zerumbet(V)</i>	<i>A. calcurata</i>	<i>A. zerumbet</i>
RT 24 h	x	√	√	x	√
90 °C 60min	x	√	√	x	√
90 °C 45min	x	√	√	√	√
90 °C 30min	x	√	√	√	√
90 °C 15min	x	√	√	x	√
60 °C 60min	x	√	√	x	√
60 °C 45min	x	√	√	√	√
60 °C 30min	x	√	√	√	√
60 °C 15min	x	√	√	x	√

**Figure 4.** Images of SEM analysis showing AgNPs of 29–68 nm. at 15.0 kV 10.3 mm × 90.0 k. 500 nm. (Images obtained using Hitachi SU6600 SEM at SLINTEC).

High resolution SEM imaging allows the analysis of size, shape and surface morphology of a sample in the nanometer range [41]. SEM analysis was performed on optimized *A.zerumbet*\_AgNP, which showed the spherical nanoparticles of average diameter between 29–68 nm as seen in **Figure 4**. A similar result was observed in the study done with the AgNPs synthesized using *Alpinia officinarum* rhizome extract which had a spherical shape and an average diameter ranging from 2.5 and 45.3 nm according to the SEM analysis [42].

### 3.3. Catalytic activity

#### 3.3.1. Photocatalytic activity

The photocatalytic activity of the synthesized AgNPs was able to degrade MO dye under solar irradiation, where the photons incidence causes a collective oscillation of electrons in the VB exciting them into the CB as shown in **Figure 5** [43]. These excited electrons result in the formation of ROS such as O<sub>2</sub> radicals and OH radicals, which



are responsible for the degradation of the MO Dye into harmless inorganic compounds like H<sub>2</sub>O and CO<sub>2</sub> [44]. The chromophore group (-N=N-) in azo dyes such as MO creates an electron deficiency along with other electrophilic components, which makes the compound less susceptible for degradation [45]. These electron deficient areas are the first to be attacked by the free radicals and the BH<sub>4</sub><sup>-</sup> ions of the catalyst NaBH<sub>4</sub>, which undergoes splitting of the Azo-bond (-N=N-) and then the benzene rings [46]. The photocatalytic degradation of dyes using just a conventional catalyst is slow and ineffective. In combination of AgNPs and NaBH<sub>4</sub>, the process is relatively fast as AgNPs makes the reaction kinetically feasible by lowering the activation energy [47]. The presumed mechanism which enhances the dye degradation massively in presence of AgNPs is with respect to the electron relay effect that aids in the transfer of electrons from the BH<sub>4</sub><sup>-</sup> ions to the dyes [48].

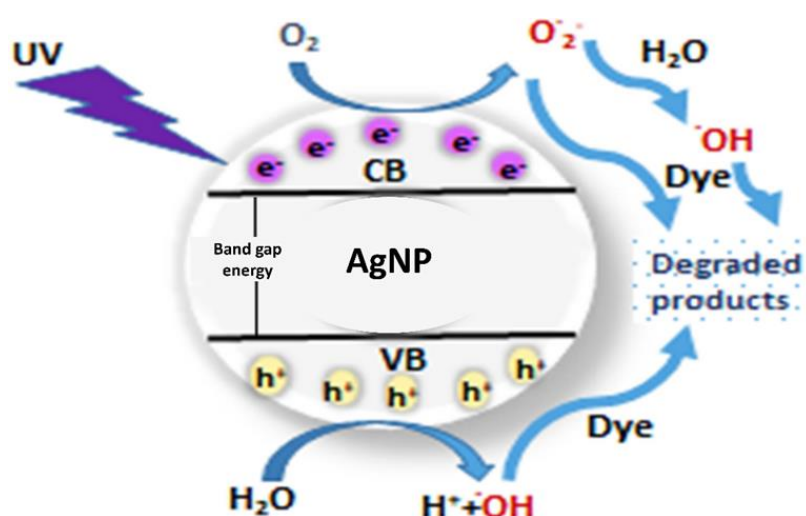


**Figure 5.** Photocatalytic degradation mechanism of dye using AgNPs upon solar irradiation, CB–Conduction band, VB–Valence band [43].

An observable degradation was not seen in all AgNP samples under sunlight without the catalyst from 0–120 m. Whereas complete degradation was observed in both concentrations of *A.calcurata*\_AgNPs and *A.zerumbet(V)*\_AgNPs with NaBH<sub>4</sub> (Figures 6 and 7). In which, *A.zerumbet(V)*\_AgNPs (4000 ppm) with NaBH<sub>4</sub> had completely degraded within 10 m (Figure 6B). The rate constant was obtained using the below equation;

$$\ln\left(\frac{C}{C_0}\right) = -kT$$

$$y = mx + c \tag{2}$$

$$mx = -kT$$

$$y = -kT + c$$

where,  $C$  = MO concentration per time interval,  $C_0$  = Initial MO concentration,  $k$  = rate constant and  $T$  = time interval. Gradient ( $m$ ) of the graph is equal to the rate constant.

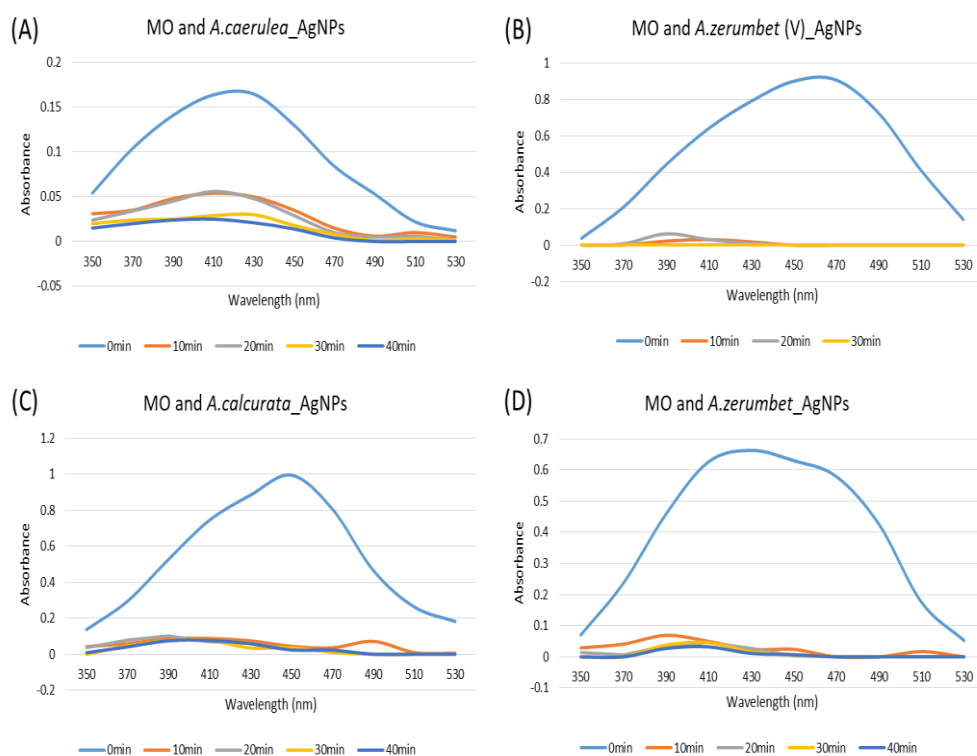


**Figure 6.** Photocatalytic degradation of MO with 4000 ppm under sunlight and NaBH<sub>4</sub> (A) *A.caerulea*\_AgNP; (B) *A.zerumbet*\_AgNP (V); (C) *A. Calcurata*\_AgNP; (D) *A.zerumbet*\_AgNP.

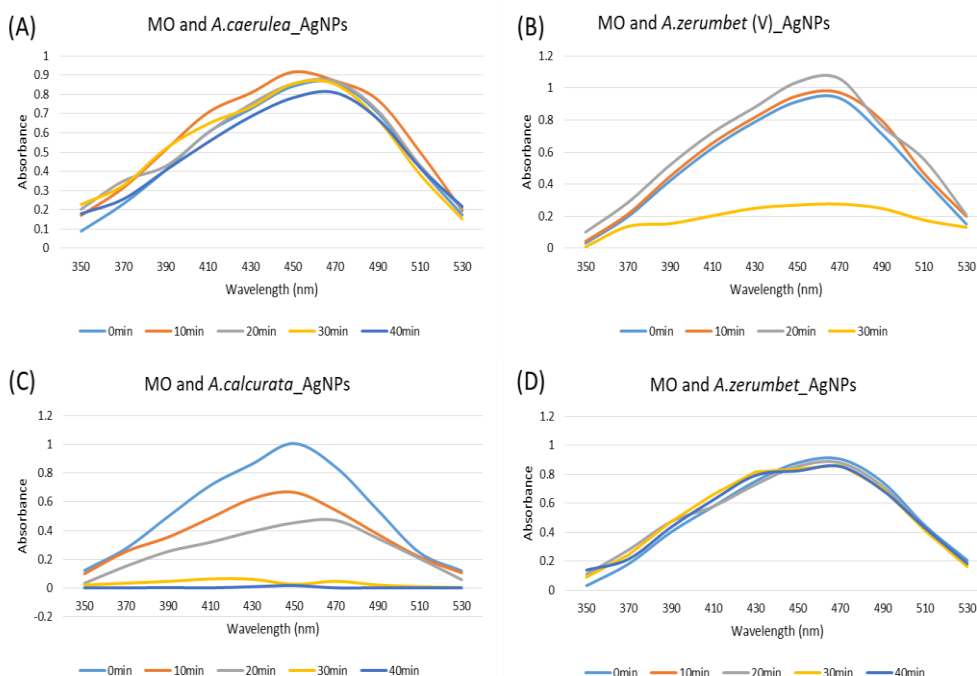


**Figure 7.** Photocatalytic degradation of MO with 267ppm under sunlight and NaBH<sub>4</sub> (A) *A.caerulea*\_AgNP; (B) *A.zerumbet*\_AgNP (V); (C) *A. Calcurata*\_AgNP; (D) *A.zerumbet*\_AgNP.

As shown in **Table 2**, the highest rate constant was observed in 4000 ppm *A.zerumbet*\_AgNP, which had a higher photocatalytic activity than other AgNP sample. 267 ppm *A.calcurata*\_AgNPs had a higher photocatalytic activity than 4000

ppm *A. calcurata*\_AgNP. A similar result of MO degradation was seen in the study conducted using AgNPs synthesized by *Terminalia arjuna* leaf extract and 1mM solution of AgNO<sub>3</sub> [49].

**Table 2.** Rate constants for photocatalytic degradation of MO.

Sample ID	4000 ppm	267 ppm
<i>A. caerulea</i> _AgNPs	0.0222	0.0012
<i>A. calcurata</i> _AgNPs	0.0783	0.0502
<i>A. zerumbet</i> _AgNPs	0.1161	0.0017

### 3.3.2. PNP degradation activity of AgNP

The reduction of PNP is not possible by NaBH<sub>4</sub> alone as conversion reaction is extremely slow due to the presence of a kinetic barrier therefore, AgNPs overcome this kinetic barrier by catalyzing the reaction and facilitating the relay of the electrons by interactive adsorption of p-nitrophenolate ions on the AgNPs surface [21]. As seen in **Figure 8** [50], the transfer of hydrogen atoms from the reducing agent (NaBH<sub>4</sub>) to the nitro group (NO<sub>2</sub>) of PNP is enhanced by AgNPs due to their high surface area and conductivity facilitating electron transfer processes [51].

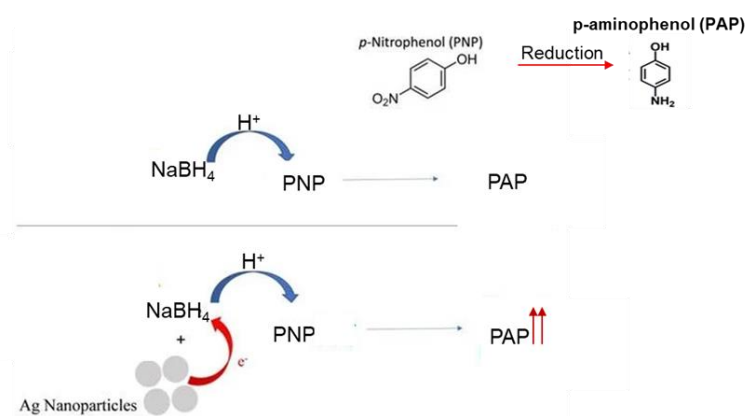


**Figure 8.** Reduction of PNP into PAP by NaBH<sub>4</sub> using AgNPs as a catalyst [50].

The importance of the AgNP catalysis action is seen in the results as there was no degradation of PNP with just NaBH<sub>4</sub> (**Figure 9**), whereas complete degradation of PNP and the formation of PAP can be seen with all AgNP samples seen in **Figures 10–13**. A study in 2019 synthesized AgNPs using *Zingiber officinale* extracts and 1 mM AgNO<sub>3</sub> showed similar degradation [52]. The rate constants were obtained using the Equation (2).

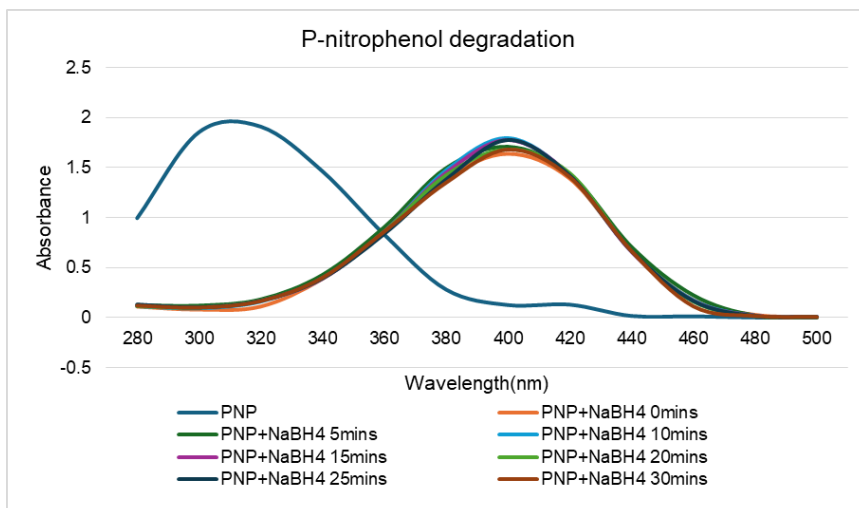


**Figure 9.** Absorbance chart showing PNP and PNP degradation with NaBH<sub>4</sub> at 5 min intervals.

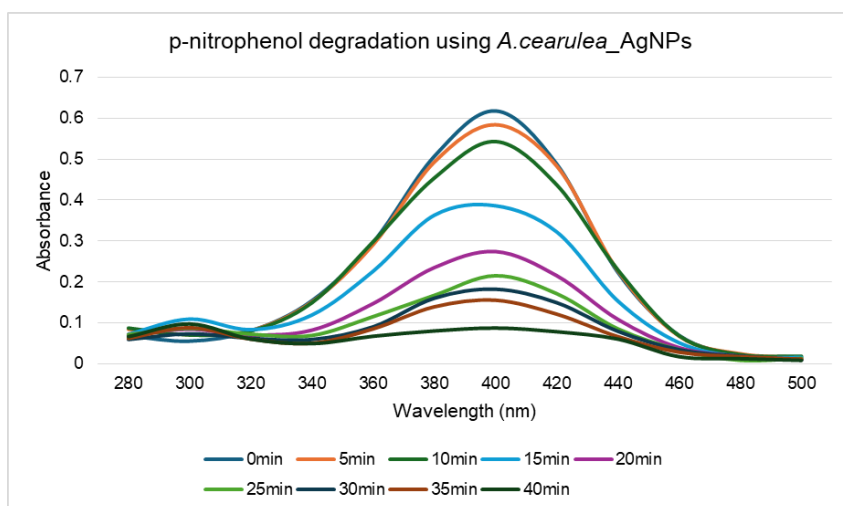


**Figure 10.** PNP degradation using NaBH<sub>4</sub> with *A.cearulea*\_AgNP at 5 min intervals.

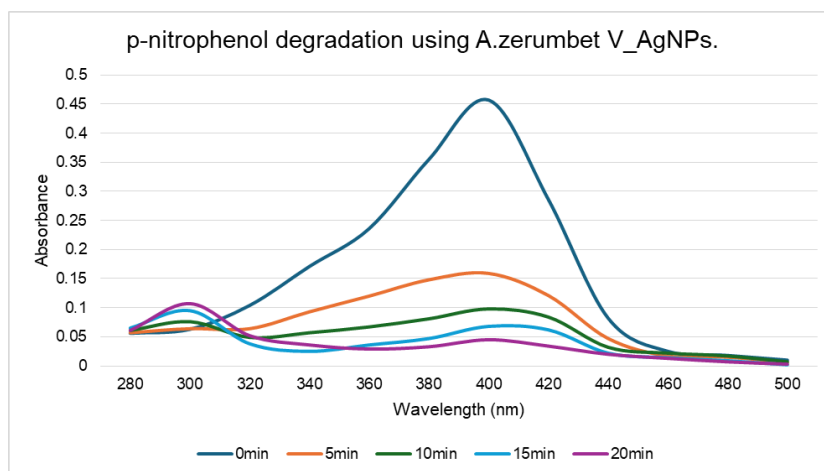


**Figure 11.** PNP degradation using NaBH<sub>4</sub> with *A.zerumbet(V)*\_AgNP at 5 min intervals.

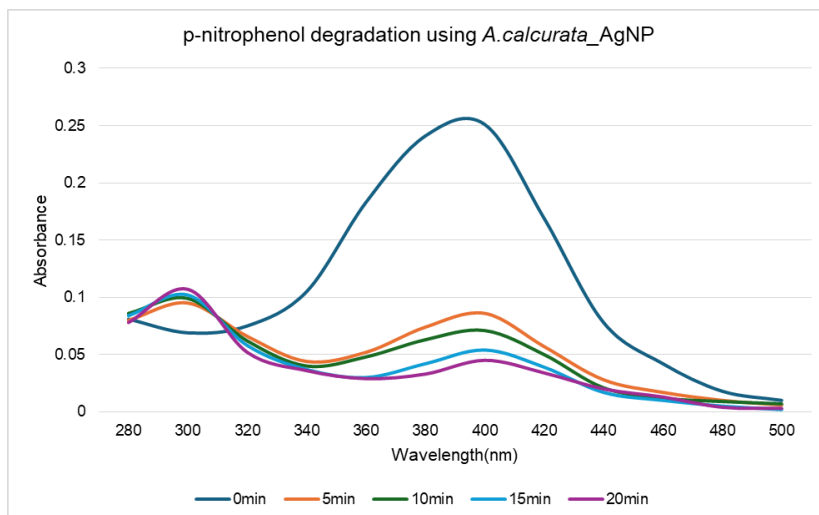


**Figure 12.** PNP degradation using NaBH<sub>4</sub> with *A.calcurata*\_AgNP at 5 min intervals.

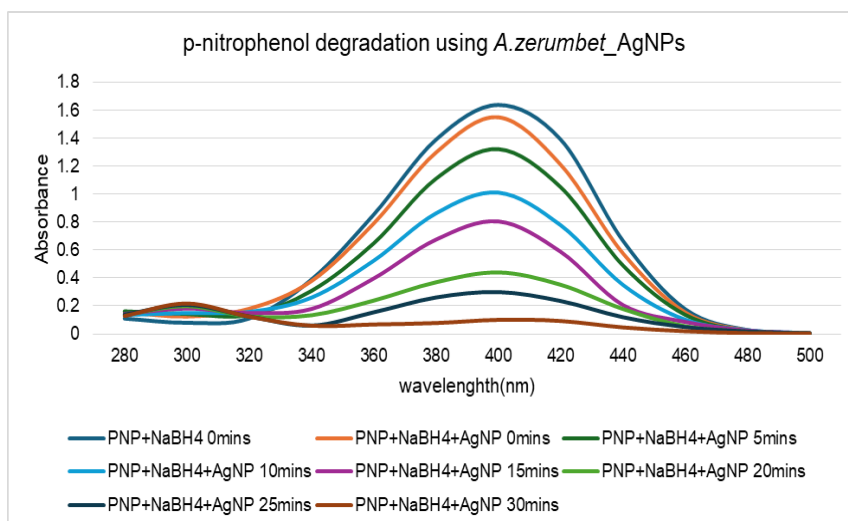


**Figure 13.** PNP degradation using NaBH<sub>4</sub> and *A.zerumbet* AgNP at 5 min intervals.

Although *A. caerulea* AgNP had the highest rate constant value of 0.9643, all the other samples showed similar rate constants indicating the high catalytic activity in the degradation of PNP as seen in **Table 3**.

**Table 3.** Rate constants for PNP degradation.

Sample	Rate constant K
<i>A.caerulea</i> _AgNPs	0.0211
<i>A.calcurata</i> _AgNPs	0.0476
<i>A.zerumbet</i> _AgNPs	0.0339
<i>A.zerumbet</i> (V)_AgNPs	0.0323

### 3.4. Cytotoxic assessment

This study demonstrated the critical function of green-synthesised nanoparticles and illuminated a route towards a more robust and sustainable future, but to fully

comprehend the potential of green-synthesised AgNPs, an evaluation of cytotoxicity is an essential step [53]. The toxicity of brine shrimps to AgNPs is seen in a dose-dependent manner, mainly due to accumulation and aggregation of AgNPs inside their gut limiting nutrient absorption and causing apoptosis due to ROS [54]. The physicochemical properties of nanomaterials, such as their particle size, shape, surface charge, and chemical composition, influence the ROS response seen in brine shrimp, leading to contrasting morphological changes and impaired biological functions [55].

For the cytotoxicity assay, the brine shrimps were grown in salt water under a yellow light and after the 24-h maturation period they were subjected to the testing on a 96 well plate. The plate was observed under a microscope for any immobile brine shrimps that are unable to swim even after gentle agitation.

All the tested shrimps were alive after 24 h in both concentrations of AgNPs (**Figures 14 and 15**). The percentage viability was calculated using the Equation (1), where all the samples showed 100% viability concluding that *Alpinia* sp. AgNP samples are non-toxic. In a study done in 2024, the brine shrimp lethality test presented significant non-toxicity of the biosynthesized AgNPs from *A. nigra* extracts and different ranges of AgNO<sub>3</sub> solutions [56].

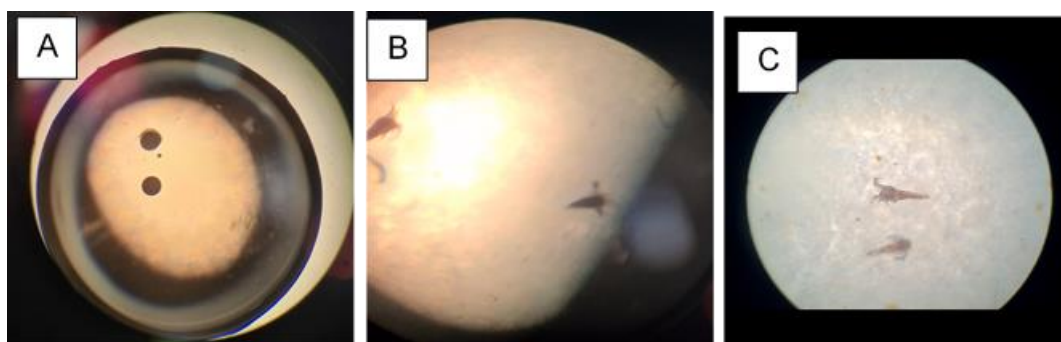


**Figure 14.** Cytotoxicity assessment of 40 mg/mL AgNPs using Brine Shrimps (A) eggs; (B) hatchlings; (C) after 24 h.

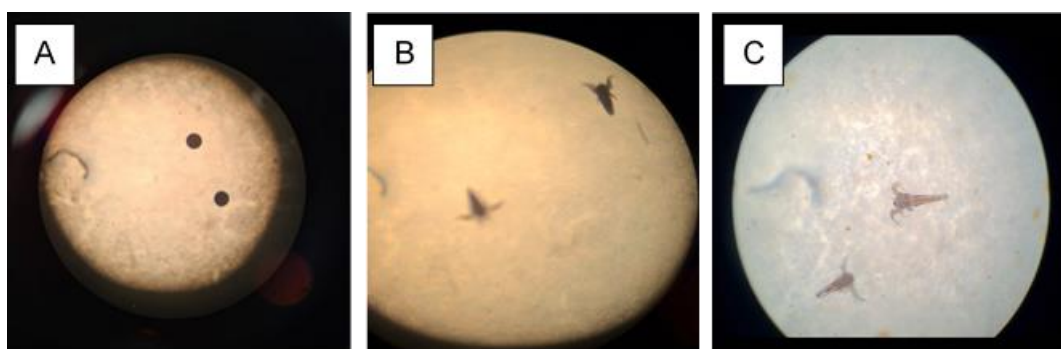


**Figure 15.** Cytotoxicity assessment of 10 mg/mL AgNPs using Brine Shrimps (A) eggs; (B) hatchlings; (C) after 24 h.

### 3.5. ABST results

According to several studies, the way that AgNPs penetrate cells, produce ROS, create free radicals, and inactivate proteins within the cell causing damage to the bacterial cell [23]. The electrostatic attraction between the negatively charged bacterial cell membrane and the positively charged AgNPs leads to this adhesion. Which

induces morphological changes that leads to impaired permeability and cell integrity where it ultimately leads to cell death due to leakage of intracellular components [57]. Once inside the bacterial cell, AgNPs causes cellular toxicity by interfering with organelle function due to generation of ROS. These ROS can also cause mutations in the Bacterial DNA and  $\text{Ag}^+$  released from AgNPs cause protein denaturation [58].

A greater antibacterial activity can be seen in *S. aureus* (**Figure 16**) compared to *E. coli* (**Figure 17**) with all the synthesized AgNPs. This suggests that Gram-positive bacteria are more sensitive to these AgNPs. A similar result was seen in a study analyzing the antibacterial activity of AgNPs synthesized using aqueous extracts of *Andrographis paniculata* stem, where the AgNPs had better activity against Gram-positive bacteria (*S. aureus*) compared to Gram-negative bacteria (*E. coli*) [59]. The presence of a thick peptidoglycan layer with abundance of pores allowing the external AgNPs to enter into the cell causing cellular damage, whereas the lipopolysaccharide layer in Gram-positive acts as a barrier leading to less penetration into the cell [60].

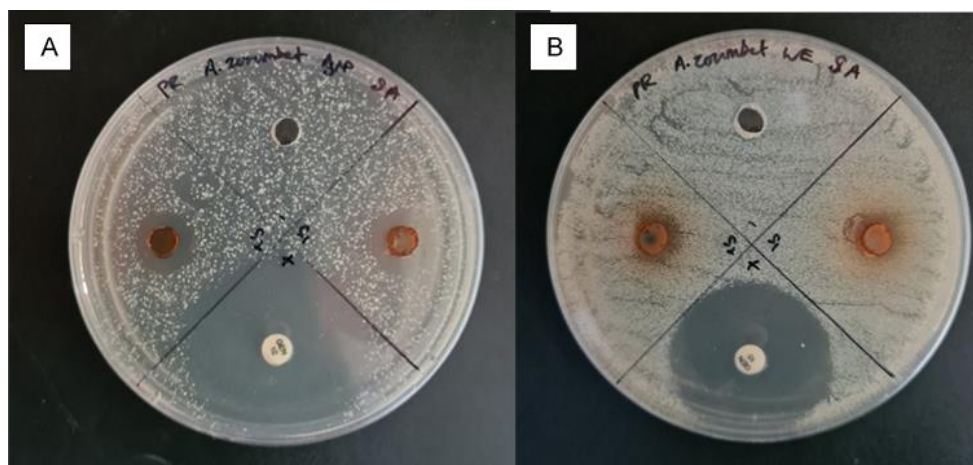


**Figure 16.** Antibacterial activity of *A.zerumbet*\_AgNP (A) and WE (B) in *S. aureus* using well diffusion.

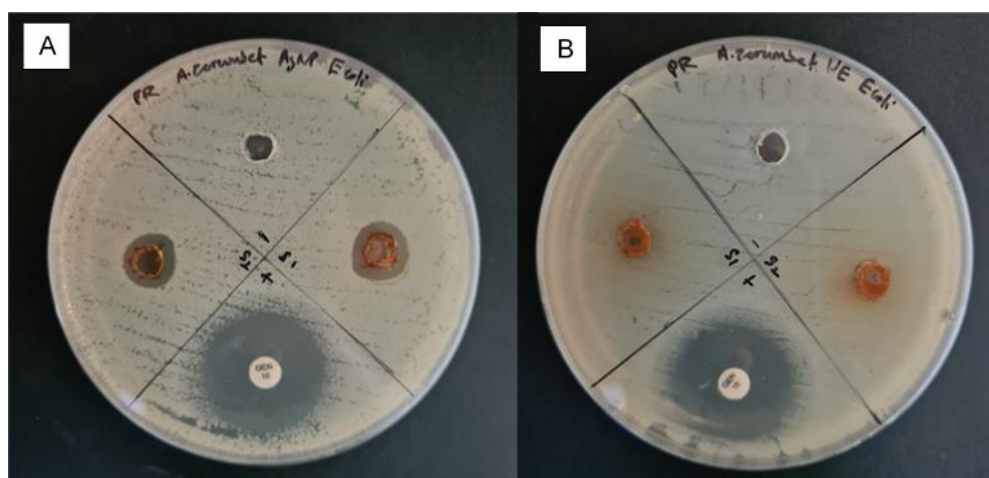


**Figure 17.** Antibacterial activity of *A.zerumbet*\_AgNP (A) and WE (B) in *E. coli* using well diffusion.

ABST of WE and AgNPs was carried out using *E. coli* and *S. aureus* in well diffusion method using gentamicin antibiotic as the positive control. **Figure 18** shows

the graphical comparison between the diameter of the ZOI by both the AgNPs and WEs in *E. coli* and *S. aureus* with respect to the gentamicin positive control. This result confirmed that AgNPs have better antibacterial activity than WEs, as out of all the WEs the ZOI was seen only in *A. zerumbet* WE in *S. aureus*. A similar ABST result was seen in a study, which is done on AgNPs synthesized using extract of *Alpinia galangal* [61].

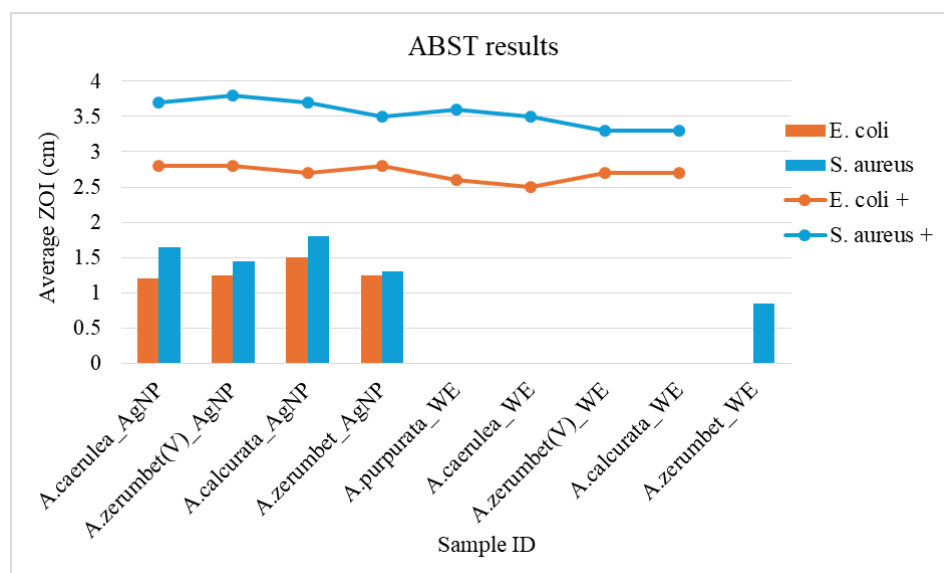


**Figure 18.** Graphical comparison of ZOI of *E. coli* and *S. aureus* for the synthesized AgNPs and the WEs with positive controls (+).

#### 4. Conclusion

In conclusion out of five, four optimized AgNP samples were successfully synthesized, at 90 °C for 30 m. SEM analysis revealed spherical shaped *A.zerumbet*\_AgNPs with 29–68 nm in size. The photocatalytic potential of AgNPs was proved by the degradation of MO dye was seen with NaBH<sub>4</sub> in all 4000 ppm AgNP samples and in two 267 ppm AgNP samples. A complete degradation was observed in *A.zerumbet(V)*\_AgNPs (4000 ppm) with NaBH<sub>4</sub> within 10 m, showing the significant photocatalytic activity of the synthesized AgNP. All the AgNPs had the capacity to catalyse PNP degradation with NaBH<sub>4</sub>, which also showed PNP does not degrade with just NaBH<sub>4</sub>. 100% viability was also seen in all AgNP samples. All the AgNPs showed antibacterial activity for both bacteria. These results indicate that highly applicable nanoparticles synthesised from *Alpinia* leaves are useful in many fields as seen with the promising results seen in removal of pollutants, also having the potential to provide a low-cost and environmentally acceptable solution. Therefore, developing and implementing green synthesis of nanomaterial in bioremediation can potentially revolutionize pollution control and management.

**Author contributions:** Conceptualization, MK; methodology, MK and RPR; software, MK and RPR; validation, MK; formal analysis, MK and RPR; investigation, MK, RPR, BG and OP; resources, MK; data curation, MK and RPR; writing—original draft preparation, RPR; writing—review and editing, MK, BG and OP; visualization,



MK and RPR, BG; supervision, MK, BG and OP; project administration, MK; funding acquisition, MK. All authors have read and agreed to the published version of the manuscript.

**Acknowledgments:** The authors acknowledge BMS for funding, the support provided by Northumbria University, UK in PNP catalysis and Institute of Nanotechnology (SLINTEC) for SEM analysis using Hitachi SU6600 SEM.

**Conflict of interest:** The authors declare no conflict of interest.

## References

1. Lu F, Astruc D. Nanocatalysts and other nanomaterials for water remediation from organic pollutants. *Coordination Chemistry Reviews*. 2020; 408. doi: 10.1016/j.ccr.2020.213180
2. Singh A, Pal D, Mohammad A, et al. Biological remediation technologies for dyes and heavy metals in wastewater treatment: New insight. *Bioresource Technology*. 2024; 343. doi: 10.1016/j.biortech.2021.126154
3. Malik S, Muhammad K, Waheed Y. Nanotechnology: A Revolution in Modern Industry. *Molecules*. 2023; 28(2): 661. doi: 10.3390/molecules28020661
4. Abid N, Khan AM, Shujait S, et al. Synthesis of nanomaterials using various top-down and bottom-up approaches, influencing factors, advantages, and disadvantages: A review. *Advances in Colloid and Interface Science*. 2022; 300: 102597. doi: 10.1016/j.cis.2021.102597
5. Singh NA, Narang J, Garg D, et al. Nanoparticles synthesis via microorganisms and their prospective applications in agriculture. *Plant Nano Biology*. 2023; 5: 100047–100047. doi: 10.1016/j.plana.2023.100047
6. Ying S, Guan Z, Ofoegbu PC, et al. Green synthesis of nanoparticles: Current developments and limitations. *Environmental Technology & Innovation*. 2022; 26: 102336. doi: 10.1016/j.eti.2022.102336
7. Kuthi NA, Basar N, Chandren S. Nanonutrition- and nanoparticle-based ultraviolet rays protection of skin. Elsevier eBooks; 2022. pp. 227–280. doi: 10.1016/b978-0-323-88450-1.00008-9
8. Zhu X, Pathakoti K, Hwang HM. Green synthesis of titanium dioxide and zinc oxide nanoparticles and their usage for antimicrobial applications and environmental remediation. *Green Synthesis, Characterization and Applications of Nanoparticles*. 2019; 223–263. doi: 10.1016/b978-0-08-102579-6.00010-1
9. Zhang Q, Zheng Y, Hu X, et al. Ethnopharmacological uses, phytochemistry, biological activities, and therapeutic applications of *Alpinia oxyphylla* Miquel: A review. *Journal of Ethnopharmacology*. 2018; 224: 149–168. doi: 10.1016/j.jep.2018.05.002
10. Kumar KM, Asish G, Sabu M, Balachandran I. Significance of gingers (Zingiberaceae) in Indian System of Medicine- Ayurveda: An overview. *Ancient Science of Life*. 2013; 32(4): 253. doi: 10.4103/0257-7941.131989
11. Priyono QAP, Yusniasari PA, Alifiansyah MRT, et al. Ethnomedical Potentials, Phytochemicals, and Medicinal Profile of *Alpinia galanga* L.: A Comprehensive Review. *BIO Integration*. 2024; 5(1). doi: 10.15212/bioi-2024-0032
12. Ray SS, Gusain R, Kumar N. Classification of water contaminants. *Carbon Nanomaterial-Based Adsorbents for Water Purification*. 2020; 11–36. doi: 10.1016/b978-0-12-821959-1.00002-7
13. de Vasconcelos GMD, Della-Flora IK, Kelbert M, et al. Screening of Azo-Dye-Degrading Bacteria from Textile Industry Wastewater-Activated Sludge. *Eng*. 2024; 5(1): 116–132. doi: 10.3390/eng5010008
14. Marimuthu S, Antonisamy AJ, Malayandi S, et al. Silver nanoparticles in dye effluent treatment: A review on synthesis, treatment methods, mechanisms, photocatalytic degradation, toxic effects and mitigation of toxicity. *Journal of Photochemistry and Photobiology B: Biology*. 2020; 205: 111823. doi: 10.1016/j.jphotobiol.2020.111823
15. Celeste J, Mohan H, Sathya PM, et al. Detoxification of p-nitrophenol (PNP) using *Enterococcus gallinarum* JT-02 isolated from animal farm waste sludge. *Environmental Research*. 2023; 231: 116289–116289. doi: 10.1016/j.envres.2023.116289
16. Kanimozhi S, Kanthimathi M. Green nanoparticles for industrially important reactions. Elsevier eBooks; 2023. pp.453–465. doi: 10.1016/b978-0-323-95921-6.00010-x
17. Ahmed EM, Khaled HE, Elsayed A. Long-term exposure to p-Nitrophenol induces hepatotoxicity via accelerating apoptosis and glycogen accumulation in male Japanese quails. *Environmental Science and Pollution Research*. 2021; 28(32): 44420–44431. doi: 10.1007/s11356-021-13806-9

18. Kuang S, Le Q, Hu J, et al. Effects of p-nitrophenol on enzyme activity, histology, and gene expression in *Larimichthys crocea*. *Comparative Biochemistry and Physiology Part C: Toxicology & Pharmacology*. 2020; 228, 108638. doi: 10.1016/j.cbpc.2019.108638
19. Xu J, Wang B, Zhang W, et al. Biodegradation of p-nitrophenol by engineered strain. *AMB Express*. 2021; 11(1). doi: 10.1186/s13568-021-01284-8
20. Chen J, Song M, Li Y, et al. The effect of phytosterol protects rats against 4-nitrophenol-induced liver damage. *Environmental Toxicology and Pharmacology*. 2015; 41: 266–271. doi: 10.1016/j.etap.2015.12.011
21. Shimoga G, Palem RR, Lee S-H, Kim S-Y. Catalytic Degradability of p-Nitrophenol Using Ecofriendly Silver Nanoparticles. *Metals*. 2020; 10(12): 1661. doi: 10.3390/met10121661
22. Bruna T, Maldonado-Bravo F, Jara P, Caro, N. Silver Nanoparticles and Their Antibacterial Applications. *International Journal of Molecular Sciences*. 2021; 22(13): 7202. doi: 10.3390/ijms22137202
23. Loo YY, Rukayadi Y, Nor-Khaizura M-A-R, et al. In Vitro Antimicrobial Activity of Green Synthesized Silver Nanoparticles Against Selected Gram-negative Foodborne Pathogens. *Frontiers in Microbiology*. 2018; 9. doi: 10.3389/fmicb.2018.01555
24. Badawy MEI, Lotfy TMR, Shawir SMS. Preparation and antibacterial activity of chitosan-silver nanoparticles for application in preservation of minced meat. *Bulletin of the National Research Centre*. 2019; 43(1). doi: 10.1186/s42269-019-0124-8
25. Parihar A, Choudhary NK, Sharma P, et al. Evaluation of Electrochemical and Antimicrobial Efficacy of Green Synthesized Silver Functionalized Reduced Graphene Oxide Nanocomposites. *Deleted Journal*. 2024. doi: 10.1007/s44174-024-00185-1
26. Liao C, Li Y, Tjong S. Bactericidal and Cytotoxic Properties of Silver Nanoparticles. *International Journal of Molecular Sciences*. 2019; 20(2): 449. doi: 10.3390/ijms20020449
27. Rajabi S, Ramazani A, Hamidi M, Naji T. *Artemia salina* as a model organism in toxicity assessment of nanoparticles. *DARU Journal of Pharmaceutical Sciences*, [online] 23(1). doi: 10.1186/s40199-015-0105-x
28. Libralatoa G, Prato E, Migliorec L, et al. A Review of Toxicity Testing Protocols and Endpoints with *Artemia* spp. *Ecological Indicators*. 2016; 69: 35–49. doi: 10.1016/j.ecolind.2016.04.017
29. Chompoo J, Upadhyay A, Fukuta M, Tawata S. Effect of *Alpinia zerumbet* components on antioxidant and skin diseases-related enzymes. *BMC Complementary and Alternative Medicine*. 2012; 12(1). doi: 10.1186/1472-6882-12-106
30. He Y, Wei F, Ma Z, et al. Green synthesis of silver nanoparticles using seed extract of *Alpinia katsumadai*, and their antioxidant, cytotoxicity, and antibacterial activities. *RSC Advances*. 2017; 7(63): 39842–39851. doi: 10.1039/C7RA05286C
31. Ganapathy Selvam G, Sivakumar K. Phycosynthesis of silver nanoparticles and photocatalytic degradation of methyl orange dye using silver (Ag) nanoparticles synthesized from *Hypnea musciformis* (Wulfen) J.V. Lamouroux. *Applied Nanoscience*. 2014; 5(5): 617–622. doi: 10.1007/s13204-014-0356-8
32. Saha P, Mahiuddin Md, Islam ABMN, Ochiai B. Biogenic Synthesis and Catalytic Efficacy of Silver Nanoparticles Based on Peel Extracts of Citrus macroptera Fruit. *ACS Omega*. 2021; 6(28): 18260–18268. doi: 10.1021/acsomega.1c02149.
33. Carballo J, Hernández-Inda ZL, Pérez P, García-Grávalos MD. A comparison between two brine shrimp assays to detect in vitro cytotoxicity in marine natural products. *BMC Biotechnology*. 2002; 2(1): p.17. doi: 10.1186/1472-6750-2-17
34. Filly A, Fabiano-Tixier AS, Louis C, et al. Water as a green solvent combined with different techniques for extraction of essential oil from lavender flowers. *Comptes Rendus Chimie*. 2016; 19(6): 707–717. doi: 10.1016/j.crci.2016.01.018
35. Roy A, Bulut O, Some S, et al. Green synthesis of silver nanoparticles: biomolecule-nanoparticle organizations targeting antimicrobial activity. *RSC Advances*. 2019; 9(5): 2673–2702. doi: 10.1039/c8ra08982e
36. Scholl JA, Koh AL, Dionne JA. Quantum plasmon resonances of individual metallic nanoparticles. *Nature*. 2012; 483(7390): 421–427. doi: 10.1038/nature10904
37. Ismail R, Mubarak T, Al-Haddad R. Surface Plasmon Resonance of Silver Nanoparticles: Synthesis, Characterization, and Applications. *J. Biochem. Tech*. 2019; 10(2): 62–64.
38. Pugazhendhi S, Kirubha E, Palanisamy PK, Gopalakrishnan R. Synthesis and characterization of silver nanoparticles from *Alpinia calcarata* by Green approach and its applications in bactericidal and nonlinear optics. *Applied Surface Science*. 2015; 357: 1801–1808. doi: 10.1016/j.apsusc.2015.09.237
39. Tarannum N, Divya K, Gautam Y. Facile green synthesis and applications of silver nanoparticles: a state-of-the-art review. *RSC Advances*. 2019; 9(60): 34926–34948. doi: 10.1039/C9RA04164H

40. Song JY, Kim BS. Rapid biological synthesis of silver nanoparticles using plant leaf extracts. *Bioprocess and Biosystems Engineering*. 2008; 32(1): 79–84. doi: 10.1007/s00449-008-0224-6
41. Hodoroaba V-D, Rades S, Salge T, et al. Characterisation of nanoparticles by means of high-resolution SEM/EDS in transmission mode. *IOP Conference Series: Materials Science and Engineering*. 2016; 109: 012006. doi: 10.1088/1757-899x/109/1/012006
42. Atmaca H, Pulat ÇÇ, İlhan S. Synthesis of silver nanoparticles using *Alpinia officinarum* rhizome extract induces apoptosis through down-regulating Bcl-2 in human cancer cells. *Biologia Futura*. 2022; 73(3): 327–334. doi: 10.1007/s42977-022-00132-5
43. Elbadawy HA, Elhusseiny AF, Hussein SM, Sadik WA. Sustainable and energy-efficient photocatalytic degradation of textile dye assisted by ecofriendly synthesized silver nanoparticles. *Scientific Reports, Nature Portfolio*. 2023. doi: 10.1038/s41598-023-29507-x
44. Ajay S, Panicker JS, Manjumol KA, Subramanian PP. Photocatalytic activity of biogenic silver nanoparticles synthesized using *Coleus Vettiveroids*. *Inorganic Chemistry Communications*. 2022; 144: 109926. doi: 10.1016/j.inoche.2022.109926
45. Sarkar S, Banerjee A, Halder U, et al. Degradation of Synthetic Azo Dyes of Textile Industry: a Sustainable Approach Using Microbial Enzymes. *Water Conservation Science and Engineering*. 2017; 2(4): 121–131. doi: 10.1007/s41101-017-0031-5
46. Kyriakopoulos J, Kordouli E, Bourikas K, et al. Decolorization of Orange-G Aqueous Solutions over C60/MCM-41 Photocatalysts. *Applied Sciences*. 2019; 9(9). doi: 10.3390/app9091958
47. Jara YS, Mekiso TT, Washe AP. Highly efficient catalytic degradation of organic dyes using iron nanoparticles synthesized with *Vernonia Amygdalina* leaf extract. *Scientific Reports*. 2024; 14(1): 6997. doi: 10.1038/s41598-024-57554-5
48. Bhankhar A, Giri M, Yadav K, Jaggi N. Study on degradation of methyl orange-an azo dye by silver nanoparticles using UV–Visible spectroscopy. *Indian Journal of Physics*. 2014; 88(11): 1191–1196. doi: 10.1007/s12648-014-0555-x
49. Raj S, Singh H, Trivedi R, Soni V. Biogenic synthesis of AgNPs employing *Terminalia arjuna* leaf extract and its efficacy towards catalytic degradation of organic dyes. *Scientific Reports*. 2020; 10(1). doi: 10.1038/s41598-020-66851-8
50. Gu S, Wunder S, Lu Y, et al. Kinetic Analysis of the Catalytic Reduction of 4-Nitrophenol by Metallic Nanoparticles. *The Journal of Physical Chemistry C*. 2014; 18618–18625. doi: 10.1021/jp5060606
51. Al-Namil DS, Khoury EE, Patra D. Solid-State Green Synthesis of Ag NPs: Higher Temperature Harvests Larger Ag NPs but Smaller Size Has Better Catalytic Reduction Reaction. *Scientific Reports*. 2019; 9(1). doi: 10.1038/s41598-019-51693-w
52. Dinda G, Halder D, Mitra A, et al. Phytosynthesis of silver nanoparticles using *Zingiber officinale* extract: evaluation of their catalytic and antibacterial activities. *Journal of Dispersion Science and Technology*. 2019; 41(14): 2128–2135. doi: 10.1080/01932691.2019.1653194
53. Arulvasu C, Jennifer SM, Prabhu D, Chandhirasekar D. Toxicity Effect of Silver Nanoparticles in Brine Shrimp *Artemia*. *The Scientific World Journal*. 2014; 1–10. doi: 10.1155/2014/256919
54. An HJ, Sarkheil M, Park HS, et al. Comparative toxicity of silver nanoparticles (AgNPs) and silver nanowires (AgNWs) on saltwater microcrustacean, *Artemia salina*. *Comparative Biochemistry and Physiology Part C: Toxicology & Pharmacology*. 2019; 218: 62–69. doi: 10.1016/j.cbpc.2019.01.002
55. Osman AI, Zhang Y, Farghali M, et al. Synthesis of green nanoparticles for energy, biomedical, environmental, agricultural, and food applications: A review. *Environmental Chemistry Letters*. 2024. doi: 10.1007/s10311-023-01682-3
56. Tongwanichniyom S, Phewrat N, Rangarikorn N, et al. Green synthesis of silver nanoparticles using mature-pseudostem extracts of *Alpinia nigra* and their bioactivities. *Green Processing and Synthesis*. 2024; 13(1). doi: 10.1515/gps-2023-0226
57. Lee SH, Jun B-H. Silver Nanoparticles: Synthesis and Application for Nanomedicine. *International Journal of Molecular Sciences*. 2019; 20(4): 865. doi: 10.3390/ijms20040865
58. Urnukhsaikhan E, Bold B-E, Gunbileg A, et al. Antibacterial activity and characteristics of silver nanoparticles biosynthesized from *Carduus crispus*. *Scientific Reports*. 2021; 11(1): 21047. doi: 10.1038/s41598-021-00520-2
59. Hossain MdM, Polash SA, Takikawa M, et al. Investigation of the Antibacterial Activity and in vivo Cytotoxicity of Biogenic Silver Nanoparticles as Potent Therapeutics. *Frontiers in Bioengineering and Biotechnology*. 2019; 7. doi: 10.3389/fbioe.2019.00239
60. Bakhtiari-Sardari A, Mashreghi M, Eshghi H, et al. Comparative evaluation of silver nanoparticles biosynthesis by two cold-tolerant *Streptomyces* strains and their biological activities. *Biotechnology Letters*. 2020; 42(10): 1985–1999. doi: 10.1007/s10529-020-02921-1

61. Imchen P, Ziekhri M, Zhimomi BK, Phucho T. Biosynthesis of silver nanoparticles using the extract of *Alpinia galanga* rhizome and *Rhus semialata* fruit and their antibacterial activity. *Inorganic Chemistry Communications*. 2022; 109599. doi: 10.1016/j.inoche.2022.109599